Regulatory Mechanisms of the Acrosome Reaction Revealed by Multiview Microscopy of Single Starfish Sperm

Ichiro Sase,* Tatsuyuki Okinaga,‡ Motonori Hoshi,‡ Gerald W. Feigenson,§ and Kazuhiko Kinosita, Jr.*

*Department of Physics, Faculty of Science and Technology, Keio University, Hiyoshi 3-14-1, Kohoku-ku, Yokohama 223, Japan; ‡Department of Life Science, Tokyo Institute of Technology, Nagatsuta, Midori-ku, Yokohama 226, Japan; and §Department of Biochemistry, Cornell University, Ithaca, New York 14853

Abstract. The acrosome reaction in many animals is a coupled reaction involving an exocytotic step and a dramatic change in cell shape. It has been proposed that these morphological changes are regulated by intracellular ions such as Ca^{2+} and H^+. We report here simultaneous visualization, under a multiview microscope, of intracellular free Ca^{2+} concentration ($[Ca^{2+}]_i$), intracellular pH (pH_i), and morphological changes in a single starfish sperm (*Asterina pectinifera*). $[Ca^{2+}]_i$ and pH_i were monitored with the fluorescent probes indo-1 and SNARF-1, respectively. The acrosome reaction was induced with ionomycin. After the introduction of ionomycin in the medium, $[Ca^{2+}]_i$ increased gradually and reached a plateau in $\sim$30 s. The fusion of the acrosomal vacuole took place abruptly before the plateau, during the rising phase. Although the speed of the $[Ca^{2+}]_i$ increase varied among the many sperm tested, exocytosis in all cases occurred at the same $[Ca^{2+}]_i$ of $\sim$2 μM (estimated using the dissociation constant of indo-1 for Ca^{2+} of 1.1 μM). This result suggests that the exocytotic mechanism in starfish sperm responds to $[Ca^{2+}]_i$ rapidly, with a reaction time of the order of one second or less. Unlike the change in $[Ca^{2+}]_i$, an abrupt increase in pH_i was observed immediately after exocytosis, suggesting the presence of a proton mobilizing system that is triggered by exocytosis. The rapid increase in pH_i coincided with the formation of the acrosomal rod and the beginning of vigorous movement of the flagellum, both of which have been proposed to be pH_i dependent. The exocytotic event itself was visualized with the fluorescent membrane probe RH292. The membrane of the acrosomal vacuole, concealed from the external medium in an unreacted sperm, was seen to fuse with the plasma membrane.

T HE acrosome reaction is a fundamental step in fertilization that allows sperm to recognize and fuse with an egg. In echinoderm the reaction is initiated by the exposure of sperm to egg jelly followed by exocytosis of the acrosomal vacuole located at the tip of the sperm head (Dan and Hagiwara, 1967). This exocytosis results in the release of vacuole contents, exposure of the vacuole membrane and polymerization of actin into an acrosomal rod. It is this newly exposed membrane that can fuse with the plasma membrane of an egg (for reviews see e.g., Tilney, 1985; Yanagimachi, 1988). Along with the conformational changes, there is an increase in the ion permeability of the sperm plasma membrane in sea urchin (Schackmann and Shapiro, 1981) and in starfish (Matsui et al., 1986a,b).

Various aspects of the ionic regulation of the acrosome reaction have been studied using isotopes and ion sensitive fluorescent probes (for reviews see e.g., Schackmann, 1989; Garbers, 1989; Hoshi et al., 1990, 1994). With few exceptions (e.g., Florman et al., 1989; Florman, 1994), the experiments were made in a cuvette containing many sperm.

Address all correspondence to Kazuhiko Kinosita, Department of Physics, Faculty of Science and Technology, Keio University, Hiyoshi 3-14-1, Kohoku-ku, Yokohama 223, Japan. Tel.: (81) 45 563 1141 (ext. 3975). Fax: (81) 45 563 1761.

The behavior of individual cells may deviate from the averaged behavior reported in these studies. Single cell measurement is highly desirable, particularly for kinetics where averaging may well obscure precise correlations among different events. We have thus attempted to image changes in ion concentrations and morphology in a single sperm under a microscope. To make temporal correlations among these changes, we used multiview microscopy (Morris, 1990; Kinosita et al., 1991) in which multiple images of an object can be observed with either single or multiple cameras simultaneously and continuously.

In this report we focus on the changes in intracellular free Ca^{2+} concentration ($[Ca^{2+}]_i$) and intracellular pH (pH_i) that have been shown to play the major roles in the acrosome reaction (see reviews above). $[Ca^{2+}]_i$ and pH_i were monitored using the fluorescent indicator dyes indo-1 (Grynkiewicz et al., 1985) and SNARF-1, respectively, and in both cases fluorescence ratios derived from pairs of emission images are analysed (Dunn et al., 1994). The acrosome reaction was induced with ionomycin, a divalent cation ionophore, because sperm on a cover-slip somehow did not respond to egg jelly efficiently. Single cell measurements have revealed that the acrosomal exocytosis takes place at a well-defined threshold value of $[Ca^{2+}]_i$ and is followed by an abrupt and rapid increase in pH_i. In addi-

tion, using the membrane probe RH292, we have succeeded in visualizing in realtime the process of the exposure of the vacuole membrane, which had been concealed behind the cell membrane, at the tip of the sperm head.

Materials and Methods

Sperm Isolation and Egg Jelly Preparation

The starfish *Asterina pectinifera* was used for experiments. Dry sperm, obtained by cutting sperm testes, was kept on ice until just before use. The dry sperm was washed with artificial seawater (ASW)[1] and diluted with ASW to appropriate concentrations just before use. Eggs were collected by treating matured ovaries with 1-methyladenine. Egg jelly solution was prepared and its concentration was determined by the method of Matsui et al. (1986a).

Seawater

Normal and Ca^{2+}-free ASW (CaFASW) were purchased from Jamarine Laboratories (Osaka, Japan). Their pH was adjusted by adding 10 mM Pipes for pH 6.80 and 10 mM EPPS for pH 8.30. 1 mM EGTA was added to CaFASW.

Oxygen-free artificial seawater was prepared by the following procedure. ASW containing 6.0 mg/ml of D-glucose was degassed under reduced pressure for 30 min. Then, glucose oxidase (Sigma Chemical Co., St. Louis, MO) and catalase (Sigma) were added to respective concentrations of 0.20 mg/ml and 0.036 mg/ml. Glucose oxidase and catalase were kept at $-80°C$ in powder form. The oxygen-free ASW was used within 2 h.

Except where stated otherwise, experiments were performed at 20°C and at pH 8.30.

Acrosome Reaction Induced with Egg Jelly

To measure the rate of acrosome reaction in individual batches, we carried out the following assay. 50 μl of a sperm suspension (0.4% dry sperm by volume) in ASW was mixed with 50 μl of an egg jelly solution (0.1 mg sugar/ml). The mixture was incubated at 20°C for 4 min, and then sperm were fixed by adding 10 μl of 8% glutaraldehyde (Polyscience Co., Warrington, PA). Reacted sperm, judged as having an acrosomal rod, were scored, under a phase-contrast microscope with an oil-immersion 100× objective, at a total magnification of 1000×. At least 100 sperm were scored at random.

Loading of Indo-1 and SNARF-1

A 50 μM solution of acetoxymethyl ester of indo-1 (indo-1AM; Dojindo Laboratories, Kumamoto, Japan) was prepared by adding a stock solution (2 mM in DMSO) to CaFASW (pH 6.80) containing 0.03% of Cremophor EL (Nacalai Tesque, Kyoto, Japan), and sonicating for 30 s (Suncleaner SC-20A, 39kHz; Tokyo, Japan). One volume of dry sperm was gently added to four volumes of the dye solution and incubated at 0°C in the dark for 18 h.

Loading of SNARF-1 was the same except Cremophor was omitted and incubation time was 10–12 h.

Staining with diI and RH292

To visualize the membrane transformation, we stained the plasma membrane of living sperm with the fluorescent probes *N*-(3-(triethylammonium)propyl)-4-(4-(*p*-dibutylaminophenyl)butadienyl)-pyridinium dibromide (RH292; Molecular Probes, Inc., Eugene, OR) or 1,1′-dioctadecyl-3,3,3′,3′-tetramethylindocarbocyanine perchlorate (diI; Molecular Probes). Staining was performed under a microscope just before measure-

ment. For both RH292 and diI, sperm were introduced in a flow chamber in advance. Then 10 μl of ASW containing 15 μM of RH292 or 250 μM of diI was introduced into the flow chamber (volume ~20 μl), and residual dye was immediately removed by infusing dye-free ASW. In the case of water-insoluble diI, the dye suspension had to be sonicated just before infusion. Less than 1% of sperm were stained with diI; presumably, those hit by a diI particle(s) were stained.

Observation Chamber

The flow chamber for observation was made of a pair of coverslips, 24 × 36 mm² for bottom and 8 × 12 mm² for top. Two parallel spacer strips were inserted to adjust the height of the chamber to ~50 μm, leaving two openings on opposite sides for perfusion. To ensure smooth flow, an antechamber with tapered height was attached to each opening by making a slant ceiling with a 8 × 12 mm² coverslip. Ionomycin flowed into the main chamber through a thin plastic tube inserted into one of the antechambers, while the other antechamber absorbed the outflow. The flow volume was about three times the chamber volume.

In experiments requiring complete deoxygenation, the entire chamber assembly was enclosed in a plexiglass box; a rectangular opening was made at the bottom of the box, on which the chamber was mounted. During observation, N_2 gas flowed through the box.

Multiview Microscopy

All results reported in this paper were obtained with a Diaphot-TMD inverted microscope (Nikon, Tokyo, Japan). The optical paths for simultaneous observation of fluorescence and phase images are diagrammed in Fig. 1. Two different fluorescence images were observed simultaneously (Kinosita et al., 1991) with an image intensifier (model KS-1381; Video Scope International, Dulles International Airport, DC) coupled to a CCD camera (model CCD-72; Dage/MTI, Michigan, IN). A separate CCD camera (model CCD-72; Dage/MTI), equipped with a 2× image magnifier, detected a phase-contrast image. Images from the two cameras were put together in one frame in a multi-viewer (model MV-24C; For. A., Tokyo, Japan) and recorded on a video recorder (model A-VS1; Toshiba, Tokyo, Japan) at the video rate of 30 frames/s. Recorded images were transmitted to a digital image processor (model C2000; Hamamatsu Photonics K.K., Hamamatsu, Japan), through a time base corrector (model FA-310; For A.), for analysis.

For triple-view microscopy of sperm loaded with indo-1, the fluorescence was excited at 340 nm, and emission between 380 nm and 560 nm was observed through a 100× objective (Nikon Fluor/1.30 oil ph4DL). The phase contrast image formed with light above 560 nm was separated from the fluorescence images with a dichroic mirror (Sigma Koki Co., Ltd., Hidaka, Saitama, Japan). The dichroic mirrors in the splitter assembly for fluorescence had a separation wavelength at 455 nm (Kawai
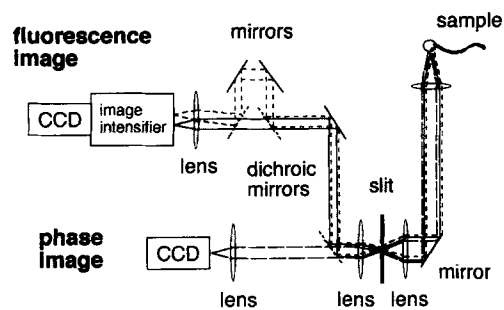
Figure 1. Optical system for simultaneous acquisition of fluorescence and phase contrast images. The excitation source for fluorescence was a 100 W mercury lamp, and a tungsten lamp was used for the phase image (not shown in the figure). Fluorescence and transmitted beams were separated with a dichroic mirror placed outside the microscope body. The fluorescence was further separated by wavelengths with a splitter assembly made of dichroic (*dotted lines*) and plane (*solid lines*) mirrors, and both images were recorded with a single CCD camera equipped with an image intensifier. The phase image was monitored with another CCD camera.

Kogaku, Shizuoka, Japan). For sperm loaded with SNARF-1, the fluorescence was excited at 540 nm and emission above 570 nm was observed through the same objective. A dichroic mirror with a separation wavelength of 455 nm (Sigma Koki) split the phase image below 455 nm from the fluorescence. The dichroic mirrors in the splitter assembly for fluorescence had a separation wavelength at 620 nm (Kawai Kogaku).

For dual-view microscopy of a sperm stained with RH292 or dil, the fluorescence was excited at 546 nm and emission above 580 nm was observed. The fluorescence was not split into components. A dichroic mirror with a separation wavelength of 455 nm was used to split fluorescence and phase (<455 nm) images.

Recorded images were corrected for distortion and shading as described (Kinosita et al., 1991).

Estimation of $[Ca^{2+}]_i$

Free calcium concentration in a cell was calculated from the relationship

$$[Ca^{2+}]_i/([Ca^{2+}]_i + K_d) = [(R - R^{free})/(R^{bound} - R^{free})] \qquad (1)$$

where K_d is the dissociation constant of indo-1 for calcium (Grynkiewicz et al., 1985) and

$$R = (I_B - \omega I_G)/(I_B + \omega I_G) \qquad (2)$$

$$\omega = (I_B^{free} - I_B^{bound})/(I_G^{bound} - I_G^{free}). \qquad (3)$$

Symbols I_B and I_G denote, respectively, the fluorescence intensities below and above 455 nm, and the superscripts free and bound refer to quantities at zero and saturating calcium concentrations. Because R depends only on the ratio between the two intensities I_B and I_G, $[Ca^{2+}]_i$ thus estimated is not influenced by the intracellular concentration of indo-1 that was not precisely controlled (Dunn et al., 1994).

To obtain the values of ω, R^{free}, and R^{bound}, calibration using homogenized sperm was carried out. Dry sperm were washed once with CaFASW (pH 6.80), and 100 mM EGTA (pH 7.9) was added to a final concentration of 0.5 mM. Then indo-1 (2.9 mM in water) was added to a final concentration of 20 μM. This suspension was carefully homogenized in the presence of 2% (vol/vol) Triton X-100 (Wako Chemicals, Osaka, Japan) until the sperm heads became indistinguishable under the microscope. After homogenization, 1 N NaOH was added to adjust the pH of the suspension to the intracellular value of 7.4–7.5 (Matsui et al., 1986a). The homogenate was then divided into halves. To one, 100 mM CaCl₂ was added dropwise, and 100 mM EGTA (pH 7.9) to the other, while monitoring and readjusting pH. Upon each dropwise addition, I_B and I_G were measured under the multiview system and corrected for a blank (homogenate without indo-1 prepared from the same batch). Limiting values were taken as I^{bound} and I^{free}. To monitor the titration process, fluorescence spectra were also measured in a fluorometer (model F-4010; Hitachi Co., Ltd., Ibaragi, Japan) using a 2 × 10 × 40 mm³ quartz cuvette placed at 45° to the excitation and emission (back surface) paths.

Photobleaching of indo-1 slightly influenced the measured value of $[Ca^{2+}]_i$ in sperm for an unknown reason: 50% bleaching resulted in an apparent reduction in $[Ca^{2+}]_i$ of 5%. In most experiments shown in Fig. 5, fluorescence intensity at the end of the experiments had decreased to about 25% of the initial value, implying an error in $[Ca^{2+}]_i$ of up to 10%. Auto-fluorescence of the sperm was low (<1%) compared to the indo-1 fluorescence.
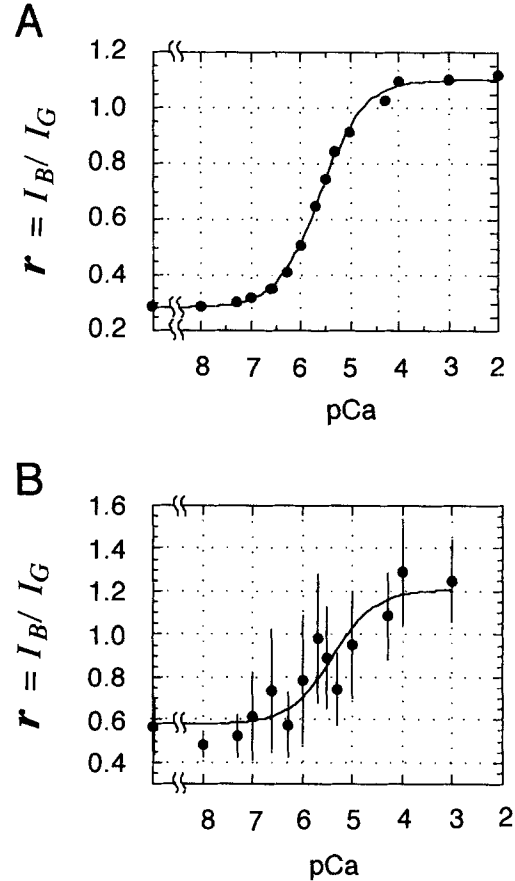
Estimation of K_d of Indo-1 for Ca^{2+}

To estimate the dissociation constant, K_d, of indo-1 for Ca^{2+} inside sperm, we attempted two sets of calibration, (a) in a buffer at a high ionic strength and (b) in situ.

(a) A series of solutions containing 225 mM KCl, 25 mM NaCl, 10 mM MOPS, 10 mM EGTA, 464 mM sucrose, and CaCl₂ at 0–11 mM, were prepared, and each was titrated with NaOH to pH 7.00 ± 0.02 at 20°C. Free calcium concentrations, $[Ca^{2+}]$, in these solutions were calculated using the dissociation constant of EGTA for calcium of 490 nM reported for a similar solution (Grynkiewicz et al., 1985). 2.5 μM of indo-1 was added (without significant change in pH), and the fluorescence intensities below and above 455 nm, I_B and I_G, were measured in an observation chamber under the multi-view system (the path for the phase image in Fig. 1 was omitted). As shown in Fig. 2 A, the ratio $r = I_B/I_G$ versus $[Ca^{2+}]$ was fitted with K_d of 1.1 μM. This value is close to the value of 1.5 μM reported by

Schackmann and Chock (1986) for a buffer approximating the ionic conditions inside sperm.

(b) Sperm loaded with indo-1 were washed and incubated in the solutions above, and 10 or 5 μg/ml of ionomycin was added to equilibrate free calcium concentrations inside and outside the sperm. After 5 min, fluorescence intensities I_B and I_G were measured for individual sperm under the multiview system (without the phase-image path). The results are shown in Fig. 2 B, which yielded a value for $(I_G^{free}/I_G^{bound}) \times K_d$ of 3.9 μM. Unlike the case with the buffer solutions above, the ratio I_G^{free}/I_G^{bound} could not be determined reliably, because absolute values of fluorescence intensity varied considerably among different sperm. The data suggested that this ratio was between 1 and 3.

In this paper, we report $[Ca^{2+}]_i$ values based on the buffer K_d of 1.1 μM

Figure 2. Estimation of K_d of indo-1 for calcium in a buffer (A) and in situ (B). The ratio $r = I_B/I_G$, where I_B and I_G are, respectively, the fluorescence intensities below and above 455 nm, is plotted against free calcium concentration (pCa = $-\log([Ca^{2+}]))$. Smooth lines are the best-fit curves for the relation $r = r^{free} + (r^{bound} - r^{free}) \times [Ca^{2+}]/\{[Ca^{2+}] + (I_G^{free}/I_G^{bound}) \times K_d\}$, where the superscripts free and bound refer to quantities at $[Ca^{2+}] = 0$ and ∞, respectively. This relation is equivalent with Eq. 1 in text. (A) The buffer consisted of 225 mM KCl, 25 mM NaCl, 10 mM MOPS, 10 mM EGTA, 464 mM sucrose, 0–11 mM CaCl₂, and 2.5 μM indo-1, and pH was titrated with NaOH to 7.00 at 20°C. Fluorescence measurement was made at 22°C. The best-fit curve was obtained at $K_d = 1.1$ μM for measured I_G^{free}/I_G^{bound} of 2.37. Individual intensities, I_B and I_G, could also be fitted with $I = I^{free} + (I^{bound} - I^{free}) \times [Ca^{2+}]/([Ca^{2+}] + K_d)$, yielding $K_d = 900$ nM for I_B and 1.2 μM for I_G, respectively. (B) Sperm loaded with indo-1 and incubated in the above buffer containing 10 or 5 μg/ml of ionomycin for 5 min. Each point represents the average over 14 sperm, the vertical bar being standard deviation. The abscissa denotes $[Ca^{2+}]$ in the extracellular solution. The best-fit curve was obtained for $(I_G^{free}/I_G^{bound}) \times K_d = 3.9$ μM. Temperature, 22°C.

above. Values based on the in situ calibration would be somewhat (up to a few times) higher, but the considerable scatter in the calibration data as well as the unproved assumption that $[Ca^{2+}]$ was really equilibrated inside and outside the sperm make this claim only a suggestion.

Results

Loading of Indo-1

To measure $[Ca^{2+}]_i$ we loaded sperm with indo-1. Sperm were incubated with an acetoxymethyl ester of indo-1 at 0°C for 18 h, at the end of which time the indo-1 concentration inside the cell became about 50 µM (estimated in the fluorometer). Unlike the case with sea urchin sperm (Schackmann and Chock, 1986), 0.03% of cremophor, added to increase the solubility of indo-1AM, was indispensable for loading of indo-1 into starfish sperm.

By the end of the incubation, more than 80% of the indo-1 inside the sperm had been converted from the acetoxymethyl ester form, which is insensitive to calcium (Grynkiewicz et al., 1985), to the active, acid form. The rate of ester hydrolysis was monitored by adding excess ionomycin (20 µg/ml) to the sperm in normal ASW and estimating the amount of the Ca^{2+}-bound (i.e., active) form from fluorescence spectra. The results indicated that the active fraction increased linearly with incubation time. We terminated the incubation after 18 h because, with starfish *Asterina pectinifera*, indo-1 started to compartmentalize after 24 h of incubation: an intensely fluorescent point appeared near the surface between the nucleus and the mitochondrion. A corresponding organelle could not be identified in the phase contrast image. (Such compartmentalization was not observed with sea urchin sperm loaded with indo-1AM nor with starfish sperm loaded with SNARF-1AM.)

In sperm loaded with indo-1, $[Ca^{2+}]_i$ was estimated to be 700 ± 260 nM ($n = 24$) in normal ASW (pH 8.3) and 720 ± 260 nM ($n = 11$) in CaFASW (pH 8.3), indicating that the ability to maintain low $[Ca^{2+}]_i$ against a concentration gradient was preserved over the loading procedure. When challenged with egg jelly, 20–40% of loaded sperm underwent an acrosome reaction, compared to 60% of the intact sperm. On the other hand, the reaction induced by ionomycin (5 µg/ml) was not affected by the loading: the proportion of reacted sperm was 50% both before and after the incubation. Loaded sperm maintained the capacity to fertilize an egg, and normal development was confirmed through the bipinnaria stage.
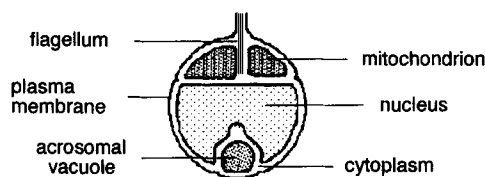
Multiview Images of Sperm Loaded with Indo-1

Fig. 3 *A* shows triple-view images of a sperm loaded with indo-1. The fluorescence images in the middle and bottom rows are used for the estimation of $[Ca^{2+}]_i$, whereas the phase contrast images in the top row reveal sperm morphology more clearly. The bright parts in the fluorescence images suggest that indo-1 localized mainly in the cytoplasm and mitochondrion of the sperm; $[Ca^{2+}]_i$ reported below refers primarily to the concentrations in these regions.

The three sets of images from left to right show a single sperm (the central sperm in the phase image) before, at the moment of, and after the acrosome reaction. In the central set of images the crevice formed by exocytosis of the acroso-

A
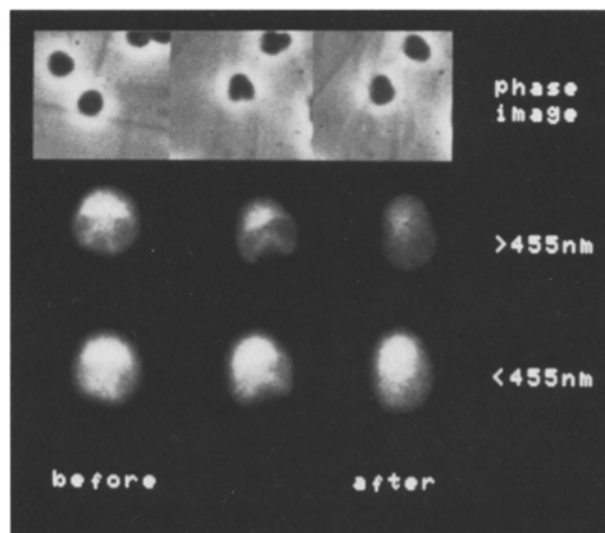
B

Figure 3. Triple-view images of a sperm loaded with indo-1. (*A*) Phase contrast images (*top*) and fluorescence images above 455 nm (*middle*) and below 455 nm (*bottom*), all observed simultaneously with the optical system in Fig. 1. The sperm at the center of the phase images is magnified in the fluorescence images. Image set at left was taken before the addition of ionomycin. The central set, taken 11 s after the addition of 5 µg/ml ionomycin, show the moment of the exocytosis of the acrosomal vacuole (note the conversion of the vacuole into a crevice). Images at right were taken 25 s after the exocytosis (36 s from the addition of ionomycin). All images were averaged over 32 frames. To compensate for the photobleaching, the fluorescence intensity in the image pairs at left, center, and right are multiplied by 1, 1.2, 1.7, respectively. (*B*) A sketch showing the structure of the sperm head before the acrosome reaction. The diameter of the head is ~2 µm.

mal vacuole is clearly seen. An acrosomal rod was observed after the reaction, though it is out of focus in the image at the top right. The fluorescence image pairs show that, as the reaction proceeded, the intensity below 455 nm became higher compared to the intensity above 455 nm, indicating an increase in $[Ca^{2+}]_i$ with time. Values of $[Ca^{2+}]_i$ were calculated pixel by pixel as described in Materials and Methods. Because ratios of the two images were used in the calculation, the effect of photobleaching was largely canceled. Detailed comparison of the morphological and calcium changes, observed simultaneously as in Fig. 3, are given below.

Morphological Changes During Acrosome Reaction

To investigate the effect of calcium, we induced the acrosome reaction with ionomycin, a divalent-cation iono-

phore. Temporal sequences of the changes in the head morphology and $[Ca^{2+}]_i$ induced by ionomycin are shown in Fig. 4. The phase contrast images in A and $[Ca^{2+}]_i$ images in B were obtained simultaneously from the same sperm. We first describe the morphological changes observed in the phase contrast images.

When sperm were introduced in a flow chamber made of untreated coverslips, some of the sperm attached to the coverslips. Nearly all of the attached sperm appeared to make contact with the glass surface at only a single point, in the head part near the partition between nucleus and mitochondrion. The tail and head continued to swing around this pivot. We usually waited for a few minutes for the vigorous movement of the flagellum to cease (-22.3 s in Fig. 4; part of the flagellum is seen at the lower right). Then we introduced ionomycin (1 μg/ml, between -13.9 and -11.8 s in Fig. 4). In Fig. 4, the resultant flow changed the orientation of the sperm such that the flagellum now pointed toward the top right (the flagellum, however, was out of focus until 0 s). At time 0, exocytosis of the acrosomal vacuole took place and a large crevice formed at the tip of the sperm head. Vacuole fusion was a very fast process and the crevice was formed within one video frame (<33 msec). In this and subsequent figures, we define time 0 as the time of exocytosis. 1–2 s after the exocytosis, the nucleus and mitochondrion started to round up and the crevice apparently became smaller. Within a second or two after the exocytosis, an acrosomal rod became noticeable (toward lower left at 1.1 s in Fig. 4) and continued to elongate for $\sim$5 s. Vigorous movement of the flagellum also started (compare images at 1.1, 2.2, and 3.3 s in Fig. 4, where the flagellum is toward the lower right) and continued for $\sim$30 s. Then, beating of the flagellum stopped. Thereafter, most sperm remained quiet without noticeable changes, except for some sperm which tended to swell.

Sperm challenged with ionomycin at 1–10 μg/ml showed similar time courses. In all cases, significant changes in sperm morphology took place at and right after the acrosomal exocytosis. Before the exocytosis, considerable time elapsed after the introduction of ionomycin ($\sim$13 s in Fig. 4), much longer than the time required for complete medium replacement ($\sim$5 s). The interval between the beginning of medium replacement and the exocytosis varied among different sperm tested, averaging 40 $\pm$ 20 s ($n = 16$). As will be shown below, this interval is the time during which $[Ca^{2+}]_i$ slowly rises to a threshold level. The existence of a long and variable lag was also observed in the jelly-induced acrosome reaction in Pisaster sperm (Tilney et al., 1978).

At higher ionomycin concentrations of 10–20 μg/ml, an increasing number of sperm failed to form an acrosomal rod although most underwent exocytosis. In CaFASW no transformation was observed even with 10 μg/ml ionomycin.

Calcium Kinetics During Acrosome Reaction

Contrary to the rapid and drastic changes in morphology, $[Ca^{2+}]_i$ increased gradually during the acrosome reaction as shown in Fig. 4 B, where all images correspond to those in Fig. 4 A. No abrupt change in $[Ca^{2+}]_i$ was observed even at the moment of exocytosis (0 s). The dotted appearance in the $[Ca^{2+}]_i$ images is due mainly to the statistical noise

in the low-intensity fluorescence images. We disregard the apparent nonuniformity and plot the average $[Ca^{2+}]_i$ in Fig. 4 C. For $K_d = 1.1$ μM (see Materials and Methods), the basal $[Ca^{2+}]_i$ (at -22.3 s) in the head part of this cell was 700 nM, which increased to 2 μM at the time of exocytosis (0 s). The increase continued through the exocytosis and reached a plateau ($\sim$5 μM) in about 20 s. $[Ca^{2+}]_i$ in the reacted sperm did not decrease after the reaction.

In Fig. 5, calcium kinetics during the acrosome reaction in 17 individual sperm are displayed on the same panel. Time 0 is the time of exocytosis for all curves. The rate of $[Ca^{2+}]_i$ increase varied greatly among different sperm. Nevertheless the calcium level at which the exocytosis took place was essentially the same (2.3 $\pm$ 0.9 μM, $n = 17$) in all transitions. This suggests that the exocytotic mechanism in starfish sperm responds rapidly to $[Ca^{2+}]_i$ with a well-defined threshold, as has been proposed for cortical granule exocytosis in sea urchin eggs (Vogel and Zimmerberg, 1992).

We do not know the reason for the variation in the rate of $[Ca^{2+}]_i$ increase. Initially we tried to control the rate of increase by varying the concentration of ionomycin. However, as seen in Fig. 5 where results with three different concentrations (1, 5, and 10 μg/ml) are displayed, higher doses of ionomycin did not necessarily accelerate the rise in $[Ca^{2+}]_i$.

The increase in $[Ca^{2+}]_i$ started during, or immediately after, the perfusion with ionomycin, which took several seconds. Thus, the lag between the addition of ionomycin and the exocytosis is the time for $[Ca^{2+}]_i$ to reach the threshold level of about 2 μM above. As noted above, variation in the lag has also been observed between the introduction of egg jelly and the exocytosis (Tilney et al., 1978). Whether this variation in the jelly-induced reaction may also result from differences in the rate of $[Ca^{2+}]_i$ rise remains to be investigated.

Changes in pH_i During Acrosome Reaction

To monitor pH_i, sperm were loaded with SNARF-1. Changes in pH_i and sperm morphology induced by ionomycin were examined with triple-view microscopy. SNARF-1, like indo-1, tended to accumulate preferentially in the mitochondrion and cytoplasm as shown in Fig. 6 A (compare with Fig. 3 B). Fig. 6 A shows fluorescence images 6.9 s before, at the moment of, and 13.5 s after exocytosis. The upper two sets of images (raw images) indicate that, upon exocytosis, the fluorescence intensity above 620 nm clearly increased relative to the intensity below 620 nm, implying an increase in pH_i, both in the mitochondrion and cytoplasm. The bottom set (ratio images) suggests that the increase was uniform inside the sperm including the mitochondrion and cytoplasm. Here again the effect of photobleaching was canceled in the ratio images.

The time course of pH_i changes averaged over the head portion is shown in Fig. 6 B. Unlike the gradual change in $[Ca^{2+}]_i$, pH_i showed an abrupt rise immediately after the exocytosis ($n = 8$). Morphological changes in SNARF-1-loaded sperm were similar to those in sperm loaded with indo-1, except that the mitochondrion and nucleus did not become spherical after the reaction.

Absolute values of pH_i could not be estimated with SNARF-1, because the fluorescence spectra of intracellu-
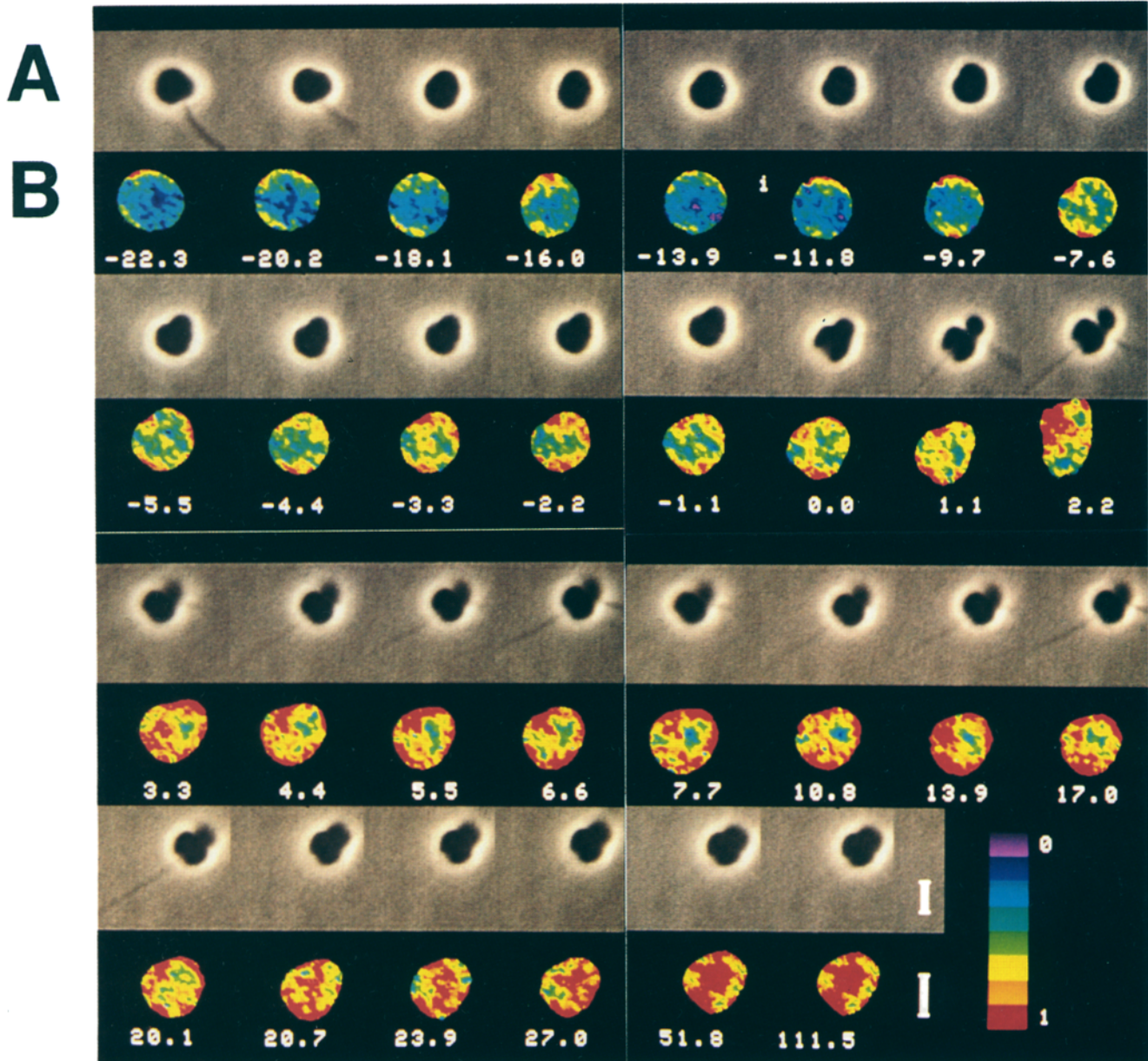
Figure 4. Ionomycin-induced changes in morphology and $[Ca^{2+}]_i$ observed simultaneously in a single sperm. (A) Phase contrast images at indicated times in seconds, time 0 being the time of acrosomal exocytosis. Each image was integrated over 16 video frames (0.53 s). ASW containing 1 μg/ml of ionomycin was introduced in the observation chamber made of a pair of coverslips between −13.9 to −11.8 s. (B) $[Ca^{2+}]_i$ estimated from indo-1 fluorescence. The quantity $[Ca^{2+}]_i/([Ca^{2+}]_i + K_d)$, where K_d is the dissociation constant of indo-1 for Ca^{2+}, is linearly color coded over the range of 0–1 as indicated in the color bar. Before the calculation, each fluorescence image was integrated over 16 frames. Bars in A and B indicate 2 μm. (C) Averaged $[Ca^{2+}]_i$ in the sperm head, calculated from B, plotted against time. The arrowhead indicates the time when ionomycin was introduced in the chamber.
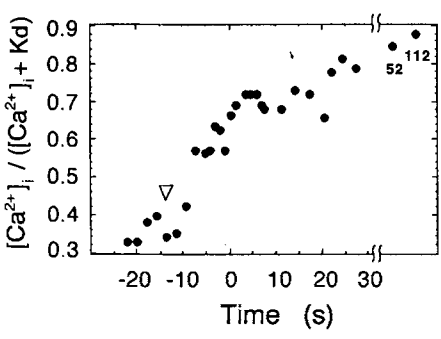
lar SNARF-1 differed from the spectra of SNARF-1 solutions. Thus, the ordinate in Fig. 6 B is given in terms of the ratio $I_{>620nm}/I_{<620nm}$ where $I_{>620nm}$ and $I_{<620nm}$ are fluorescence intensities above and below 620 nm. When SNARF-1 in solution was titrated, this ratio changed from 0.29 at pH <6 to 1.00 at pH >10 (see scale bar on the right). Although quantitative analysis is impossible, the sizable change in Fig. 6 B, compared to the solution range above,
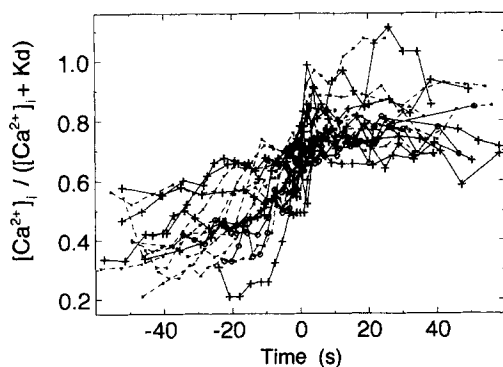
Figure 5. Changes in $[Ca^{2+}]_i$ during acrosome reaction in 17 individual sperm. The reaction was induced with ionomycin at 1 µg/ml (*open circles with solid line, n* = 2), 5 µg/ml (*dots with dashed line, n* = 10), or 10 µg/ml (*crosses with solid line, n* = 5). Calcium levels were estimated from fluorescence images as in Fig. 4 and averaged within the head portion. At time 0 (the moment of exocytosis), $[Ca^{2+}]_i/([Ca^{2+}]_i + K_d)$ was 0.67, on the average, corresponding to $[Ca^{2+}]_i$ of 2.3 µM for K_d of 1.1 µM.

suggests that the exocytosis was followed by a large increase in pH_i.

In some sperm, a small and slow increase in pH_i was observed before the exocytosis (at most an increase of 0.05 in the intensity ratio). This could be a side effect of ionomycin, which has been shown to catalyze electroneutral exchange of Ca^{2+} for $2H^+$ (Kauffman et al., 1980). The large increase after the exocytosis, however, cannot be ascribed to this effect, because a corresponding, abrupt rise is absent in the $[Ca^{2+}]_i$ records (Figs. 4 *C* and 5). For the same reason, the large increase in pH_i cannot be the result of membrane rupture that might be anticipated during the exocytotic events.

Exposure of the Vacuole Membrane

To observe closely the process of acrosomal exocytosis, we stained sperm with RH292, an amphiphilic dye which fluoresces intensely when bound to membranes. Because the positively charged dye does not readily cross a membrane, only the outermost membrane, the plasma membrane, was stained in unreacted sperm, as seen at the top left in Fig. 7. At −15 s, 5 µg/ml of ionomycin was introduced in the me-
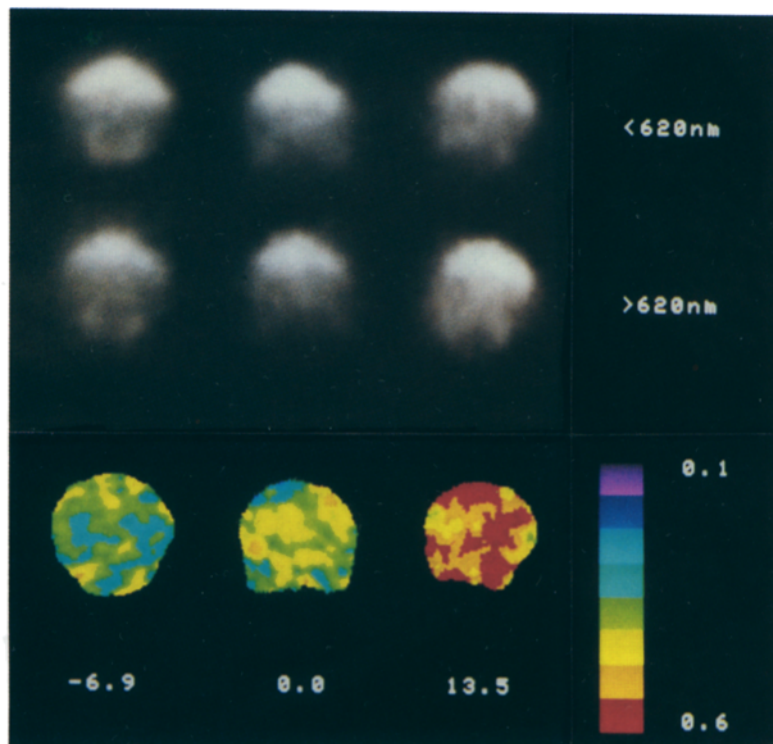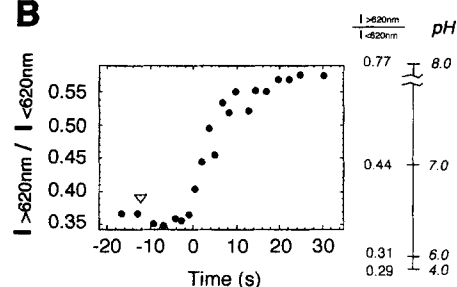

Figure 6. Typical pH_i change during an acrosome reaction induced with ionomycin. (*A*) Fluorescence images (*top,* <620nm; *middle,* >620nm) of the head part of a sperm 6.9 s before (*left*), at the moment of (*center*), and 13.5 s after (*right*) the exocytosis. All images are averaged over 16 video frames and, to compensate for the photobleaching, the fluorescence intensity in the image pairs at −6.9, 0, and 13.5 s are multiplied by 1, 1.04, 1.36, respectively. For clarity, images in the middle row are further multiplied by 2. Thus, a comparison of intensities can be made only between the upper two fluorescence images in each row. Bottom is the ratio (>620nm/<620nm) image of the same sperm. The ratio images are linearly color coded over the range of 0.1 to 0.6 as indicated in the color bar. Mitochondrion is toward the top and the acrosomal vacuole toward the bottom. (*B*) The ordinate is the intensity ratio of SNARF-1 fluorescence above and below 620 nm, averaged over the head portion; higher values indicate higher pH_i. Time 0 is the time of exocytosis, and the arrowhead indicates the addition of ionomycin (5 µg/ml). Scale bar on the right shows the relation between the intensity ratio and pH for SNARF-1 in water (pK = 7.6).

dium. Exocytosis took place at time 0, leading to the formation of an opening at the tip of the sperm head as seen in Fig. 7. The discontinuity of the fluorescent membrane at the opening, however, should only be an apparent one, in view of the absence of any Ca^{2+} inrush at the moment of exocytosis. In fact, the fluorescent plasma membrane was now continuous with the yet unstained membrane of the acrosomal vacuole, as is evident in the next image in which the vacuole membrane was also stained with RH292. The source of RH292 for the vacuole membrane should be either residual RH292 in the medium or lateral diffusion from the plasma membrane. In either case, the implication is that the inner surface of the vacuole membrane was now accessible to external RH292, and thus the surface hitherto concealed from the external medium was now exposed. The newly exposed membrane started to elongate into an acrosomal rod as seen in the bottom images in Fig. 7. This acrosomal rod elongated more than 10 μm. Sperm stained with RH292 had a tendency to swell and breakdown after the acrosome reaction, even in the absence of excitation light.

Discussion

Studies on echinoderm sperm, particularly in sea urchins, have revealed much about the ionic regulation of the acrosome reaction (Tilney, 1985; Schackmann, 1989; Gar-
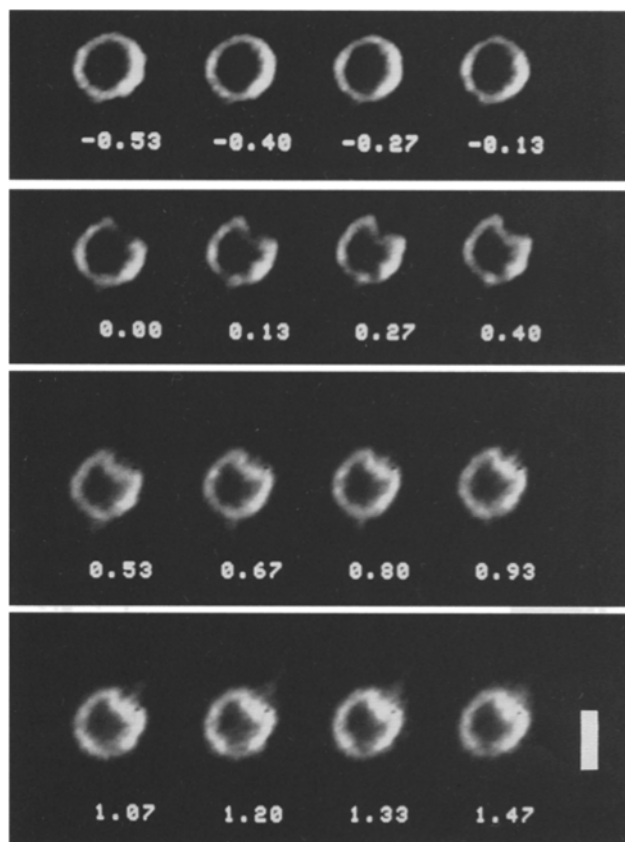
Figure 7. Sequential fluorescence images showing the time course of acrosomal exocytosis in a sperm stained with RH292. Time in seconds. Ionomycin (5 μg/ml) was introduced at −15 s. Each image was integrated over four frames. Bar, 2 μm.

bers, 1989; Hoshi et al., 1990, 1994). The requirements for external Ca^{2+} (Dan, 1954; Collins and Epel, 1977) and an increase in pH_i (Tilney et al., 1978; Schackmann et al., 1978) have led to the general consensus that the increases in $[Ca^{2+}]_i$ and pH_i are the two key factors of the acrosome reaction. Tilney et al. (1978) have put forward the idea that the increase in $[Ca^{2+}]_i$ is responsible for acrosomal exocytosis and the increase in pH_i for the polymerization of actin into the acrosomal rod. If this idea is basically correct, the complex mechanism of the acrosome reaction is split into two broad categories: (*a*) how egg jelly, or its components, induces the required ionic changes, and (*b*) how Ca^{2+} and pH respectively cause the exocytosis and the elongation of an acrosomal rod. Our results on $[Ca^{2+}]_i$ kinetics shed some light on (*b*), the mechanism of exocytosis. The abrupt rise of pH_i (Fig. 6 *B*) is consistent with Tilney's proposal. At the same time, the remarkable coincidence between the pH_i rise and exocytosis suggests the possibility that the exocytosis was the trigger for the pH_i rise, pointing to an interplay between *a* and *b*. Before discussing these topics, we first compare the ionomycin-induced reaction with the natural acrosome reaction.

Acrosome Reaction Induced with Ionomycin

In this study, we used the calcium ionophore, ionomycin, to induce an acrosome reaction. Divalent-cation ionophores such as A23187 have been widely used to induce an acrosome reaction resembling the jelly-induced reaction (Schroeder and Christen, 1982; Tilney and Inoué, 1982), although differences do exist (Tilney et al., 1978; Watson et al., 1992).

In our observation, morphological changes induced by ionomycin (Fig. 4 *A*) were quite similar to the changes in the jelly-induced reaction, including the order and timing. In both reactions, the exocytosis was rapid (<33 ms) and immediately followed by the disappearance of the exocytotic crevice and the elongation of an acrosomal rod. Within 1–2 s after the exocytosis, the nucleus and mitochondrion started to round up and this process continued for a few seconds. A noticeable difference was the final length of the acrosomal rod, which tended to be shorter (5–10 μm) with ionomycin than with jelly (~20 μm). Another difference was that jelly immediately induced vigorous flagellar movement whereas with ionomycin the activation was observed only after the exocytosis.

Thus, the essential components of the acrosome reaction, the exposure of the vacuole membrane and its protrusion into an acrosomal rod, appear to proceed in much the same way whether the initial trigger is jelly or ionomycin. This, however, does not imply that reactions prior to these two events are also the same. In particular, the kinetics of Ca^{2+} entry may well be different, because the membrane remains permeable to Ca^{2+} in the presence of ionomycin.

Role of Ca^{2+}

As shown in Fig. 4, ionomycin induced a gradual rise in $[Ca^{2+}]_i$ from a basal concentration of 700 nM (0.6 × K_d) to 6 μM (5 × K_d), and the acrosomal exocytosis occurred at about 2 μM (2.1 × K_d). These values depend on the choice of K_d (= 1.1 μM) and are underestimates if actual K_d in-

side sperm is higher (by a factor up to 2–3) as discussed in Materials and Methods.

When the uncertainties in the dissociation constants of Ca^{2+}-probes are taken into account, the threshold concentration for exocytosis above is of similar magnitude to the maximal $[Ca^{2+}]_i$ in the natural acrosome reaction, where, in sea urchins, the maximum is attained within 10 s after the addition of jelly or its major components: [3-5] $\times$ K_d (indo-1; Schackmann, 1989), 1–2 μM (K_d for indo-1 = 1.5 μM, K_d for fura-2 = 770 nM; Trimmer et al., 1986) or $\sim$1 μM (K_d for fura-2 = 250 nM; Guerrero and Darszon, 1989a) in the sea urchin Strongylocentrotus purpuratus; about 1 μM (K_d for quin 2 = 115 nM; González-Martínez et al., 1992) in the sea urchin Lytechinus pictus; $\sim$300 nM (K_d for fura-2 = 225 nM; Florman et al., 1989) in boar sperm where the increase was slower compared to echinoderms. The latency in the jelly-induced acrosome reaction may also be accounted for by the rise time of $[Ca^{2+}]_i$.

In the experiments in Fig. 5, the acrosomal exocytosis occurred at the same $[Ca^{2+}]_i$ in spite of the large variation in the rate of $[Ca^{2+}]_i$ increase. This strongly suggests that the exocytotic mechanism in starfish sperm responds to $[Ca^{2+}]_i$ and that the response is rapid (within $\sim$1 s). If the exocytosis is induced by a side effect(s) of ionomycin other than the elevation of $[Ca^{2+}]_i$, or if a long chain of reactions are involved between the sensing of $[Ca^{2+}]_i$ elevation and exocytosis, the coincidence in Fig. 5 would not have been observed. In synaptic terminals, the exocytotic mechanism responds to $[Ca^{2+}]_i$ at a rate of $\sim$3000 s^{-1} (Heidelberger et al., 1994).

The Ca^{2+} sensor for the exocytotic mechanism is characterized by a dissociation constant for Ca^{2+} of $\sim$2 μM. The presence of the relatively well-defined threshold (Fig. 5) implies that the sensor has multiple binding sites or that a number of sensors act cooperatively to induce the acrosomal exocytosis. Multiple binding has been indicated for activation of synaptic vesicle fusion (Heidelberger et al., 1994). In this system, the minimum $[Ca^{2+}]_i$ required was considerably higher (10–20 μM), reflecting the need for the microsecond response. Exocytosis at micromolar concentrations of Ca^{2+} has been reported in many other systems, including the fusion of cortical granules at fertilization in echinoderm eggs (Jaffe, 1985; Vogel and Zimmerberg, 1992; Suzuki et al., 1995). Although the machinery of vesicle fusion now appears to be basically similar among eukaryotes (Fero-Novick and Jahn, 1994), the nature of the Ca^{2+} sensor that triggers the machinery is not yet clear. Calmodulin antagonists inhibited acrosome reaction in sea urchin sperm, but the target appeared to be a Ca^{2+} channel (Guerrero and Darszon, 1989a). Proteins on exocytotic vesicles have been implicated for the cortical granule exocytosis in sea urchin eggs (Vogel and Zimmerberg, 1992). In neural systems, synaptotagmin that binds Ca^{2+} may play the role of the trigger (DeBello et al., 1993). Annexins, of which at least some respond to Ca^{2+} at $\sim$1 μM, may trigger the membrane fusion by drawing two membranes together (Creutz, 1992). In this regard, we note that Ca^{2+} alone at a micromolar concentration can induce contact of two lipid bilayers by bridging head groups of phosphatidylserine in opposing bilayers (Feigenson, 1986, 1989).

The suggestion that the exocytotic mechanism in starfish sperm responds to $[Ca^{2+}]_i$ is in apparent contradiction to the observation, in sea urchin sperm that an increase in $[Ca^{2+}]_i$ without accompanying rise in pH$_i$, either with an antibody (Trimmer et al., 1986) or by an artificial depolarization (González-Martínez et al., 1992), failed to induce an acrosome reaction. The exocytotic mechanism may operate only at an elevated pH$_i$ or only after being pretriggered by rising pH$_i$. Ionomycin in fact caused, in some sperm, a small increase in pH$_i$ before the exocytosis, although its significance is unclear because the effect was not detected in other sperm (Fig. 6 B). In starfish, an increase in pH$_i$ (as monitored with 9-aminoacridine) may not be absolutely obligatory for triggering an acrosome reaction (Hoshi et al., 1988).

Rise in pH$_i$

Egg jelly induces a rise in pH$_i$, which is an essential component of the acrosome reaction (Tilney et al., 1978; Schackmann et al., 1981; Garcia-Soto et al., 1985; Matsui et al., 1986b). Both polymerization of actin inside the acrosomal rod (Tilney et al., 1978) and the activity of dynein ATPase in the flagellum (Christen et al., 1982) are pH$_i$ dependent. In sea urchin, a rapid ($\sim$5 s) and sustained elevation of pH$_i$ by $\sim$0.2 pH unit has been observed upon addition of jelly (Schackmann et al., 1981; Guerrero and Darszon, 1989b). In starfish including A. pectinifera, Matsui et al. (1986b) detected, with 9-aminoacridine as a probe, a transient increase in pH$_i$ of 0.06 followed by a larger and sustained decrease by 0.2–0.3 pH unit.

We observed that the rise in pH$_i$ immediately after exocytosis (Fig 6 B) was coincident with the formation of an acrosomal rod and the initiation of vigorous flagellar motility, in accordance with the suggested roles of pH$_i$ for these activities. We note, however, that such an abrupt rise that is synchronous with exocytosis has not so far been documented in either jelly-induced or artificial acrosome reactions. We suspect that a sharp rise occurring asynchronously in many sperm might have been buried and unnoticed in an averaged signal obtained in a cuvette measurement.

Abrupt alkalinization occurred also in mitochondrion as seen in Fig. 6 A, implying that protons would be ejected from the mitochondrion. The tendency toward cytoplasmic reacidification which starts immediately after an acrosome reaction and which requires Ca^{2+} (Christen et al., 1983; Matsui et al., 1986b) might be related to this process. Note, however, that cytoplasmic acidification would not necessarily follow because protons released from the mitochondrion might be carried through to the extracellular space. In fact, Fig. 6 A indicates that the cytoplasm, at least the part surrounding the acrosomal vacuole, underwent alkalinization rather than acidification.

The kinetics shown in Fig. 6 B strongly suggests the presence of a proton-mobilizing mechanism that is triggered by acrosomal exocytosis or by a process that immediately precedes the exocytosis. A possibility might be a proton translocating system residing in the membrane of the acrosomal vacuole. The exposure of the vacuole membrane might activate this system and lead to cytoplasmic alkalinization, which in turn might mobilize mitochondrial protons. Further studies are needed to clarify the mechanisms underlying the observed pH kinetics.

Sase et al. Acrosome Reaction in Single Starfish Sperm

971

Acrosomal Exocytosis

At present, our understanding of the behavior of the sperm membranes is based mainly upon electron microscopic images (Dan and Hagiwara, 1967; Sardet and Tilney, 1977; Epel and Vacquire, 1978). To visualize the membrane conformational change in a living cell, we stained the outermost membrane of the sperm with the membrane probe RH292. Images such as the one at time 0 in Fig. 7 suggest that membrane fusion does not occur at many places, and a wide opening forms at the tip of the sperm head. Careful examination of sequential images gave an impression that the opening was formed by retreat of the fused membrane toward the periphery rather than by vesiculation (Dan and Hagiwara, 1967), although the latter may have been undetectable in the dim fluorescence images.

Whether the newly exposed vacuole membrane was physically connected to the plasma membrane is not clear in Fig. 7, because the water-soluble RH292 may have stained the vacuole membrane from the aqueous phase. However, when we stained the plasma membrane with a more hydrophobic dye, dil, and induced an acrosome reaction, the dye stained the newly exposed vacuole membrane as rapidly as RH292, presumably by lateral diffusion (data not shown). Connection without a barrier was established between the two membranes.

Concluding Remarks

Because the acrosome reaction is inherently variable in its time course and cannot be synchronized, a precise correlation between two (or more) events such as are shown in Figs. 5 and 6 can only be obtained by single cell measurements. In this study, we focused mainly on the exocytotic step by inducing the reaction with ionomycin. The major findings were the presence of a well-defined threshold $[Ca^{2+}]_i$ for exocytosis and the abrupt rise of pH_i following exocytosis. Signals upstream from the calcium-induced exocytosis, however, should be analyzed using egg jelly, of which essential components have been identified and purified in starfish (Hoshi et al., 1990, 1994). Single cell studies using purified components are expected to clarify complicated interplays among various signals.

Note Added in Proof: Recently, Castellano et al. (1995) have shown that, in sea urchin, the minimal Ca^{2+} concentration needed for inducing maximal number of sperm to undergo the acrosome reaction was ~ 1 μM.

References

Castellano, L. E., J. López-Godínez, G. Aldana, M. Barrios-Rodiles, A.

Obregón, L. de De la Torre, A. Darszon, and García-Soto. 1995. The acrosome reaction in digitonin-permeabilized sea urchin sperm in the absence of the natural inducer. *Eur. J. Cell Biol.* 67:23–31.

Christen, R., R. W. Schackmann, and B.M. Shapiro. 1982. Elevation of the intracellular pH activates respiration and motility of sperm of the sea urchin *Strongylocentrotus purpuratus. J. Biol. Chem.* 257:14881–14890.

Christen, R., R. W. Schackmann, and B. M. Shapiro. 1983. Metabolism of sea urchin sperm: interrelationship between intracellular pH ATPase activity and mitochondrial respiration. *J. Biol. Chem.* 258:5392–5399.

Collins, F., and D. Epel. 1977. The role of calcium ions in the acrosome reaction of sea urchin sperm: regulation of exocytosis. *Exp. Cell Res.* 106:211–222.

Creutz, C. E. 1992. The annexins and exocytosis. *Science (Wash. DC).* 258:924–931.

Dan, J. C. 1954. Studies on the acrosome. III. Effect of calcium deficiency. *Biol. Bull.* 107:335–350.

Dan, J. C., and Y. Hagiwara. 1967. Studies on the acrosome. IX. Course of acrosome reaction in the starfish. *J. Ultrastruct. Res.* 18:562–579.

DeBello, W. M., H. Betz, and G. J. Augustine. 1993. Synaptotagmin and neurotransmitter release. *Cell.* 74:947–950.

Dunn, K. W., S. Mayor, J. N. Myers, and F. R. Maxfield. 1994. Applications of ratio fluorescence microscopy in the study of cell physiology. *FASEB (Fed. Am. Soc. Exp. Biol.) J.* 8:573–582.

Epel, D., and V. D. Vacquier. 1978. Membrane fusion events during invertebrate fertilization. *Cell. Surf. Rev.* 5:1–63.

Feigenson, G. W. 1986. On the nature of calcium ion binding between phosphatidylserine lamellae. *Biochemistry.* 25:5819–5825.

Feigenson, G. W. 1989. Calcium ion binding between lipid bilayers: the four-component system of phosphatidylserine, phosphatidylcholine, calcium chloride, and water. *Biochemistry.* 28:1270–1278.

Ferro-Novick, S., and R. Jahn. 1994. Vesicle fusion from yeast to man. *Nature (Lond.).* 370:191–193.

Florman, H. M., R. M. Tombes, N. L. First, and D. F. Babcock. 1989. An adhesion-associated agonist from the zona pellucida activates G protein-promoted elevations of internal Ca^{2+} and pH that mediate mammalian sperm acrosomal exocytosis. *Dev. Biol.* 135:133–146.

Florman, H. M. 1994. Sequential focal and global elevations of sperm intracellular Ca^{2+} are initiated by the zona pellucida during acrosomal exocytosis. *Dev. Biol.* 165:152–164.

Garbers, D. L. 1989. Molecular basis of fertilization. *Annu. Rev. Biochem.* 58:719–742.

Garcia-Soto, J., L. de De La Torre, and A. Darszon. 1985. Increasing intracellular pH of sea urchin sperm with NH_4Cl induces Ca^{2+} uptake and acrosome reaction in the absence of egg jelly. *FEBS Lett.* 190:33–36.

González-Martínez, M. T., A. Guerrero, E. Morales, L. de De La Torre, and A. Darszon. 1992. A depolarization can trigger Ca^{2+} uptake and the acrosome reaction when preceded by a hyperpolarization in *L. pictus* sea urchin sperm. *Dev. Biol.* 150:193–202.

Grynkiewicz, G., M. Poenie, and R. Y. Tsien. 1985. A new generation of Ca^{2+} indicator with greatly improved fluorescence properties. *J. Biol. Chem.* 260:3440–3450.

Guerrero, A., and A. Darszon. 1989a. Egg jelly triggers a calcium influx which inactivates and is inhibited by calmodulin antagonists in the sea urchin sperm. *Biochim. Biophys. Acta.* 980:109–116.

Guerrero, A., and A. Darszon. 1989b. Evidence for the activation of two different Ca^{2+} channels during the egg jelly-induced acrosome reaction of sea urchin sperm. *J. Biol. Chem.* 264:19593–19599.

Heidelberger, R., C. Heinemann, E. Neher, and G. Matthews. 1994. Calcium dependence of the rate of exocytosis in a synaptic terminal. *Nature (Lond.).* 371:513–515.

Hoshi, M., T. Matsui, I. Nishiyama, T. Amano, and Y. Okita. 1988. Physiological inducers of the acrosome reaction. *In* Regulatory Mechanisms in Developmental Processes. G. Eguchi, T. T. Okada, and L. Saxen editors. Elsevier, Dublin. 19–24.

Hoshi, M., T. Amano, Y. Okita, T. Okinaga, and T. Matsui. 1990. Egg signals for triggering the acrosome reaction in starfish spermatozoa. *J. Reprod. Fert. Suppl.* 42:23–31.

Hoshi, M., T. Nishigaki, A. Ushiyama, T. Okinaga, K. Chiba, and M. Matsumoto. 1994. Egg-jelly signal molecules for triggering the acrosome reaction in starfish spermatozoa. *Int. J. Dev. Biol.* 38:167–174.

Jaffe, L. F. 1985. The acrosome reaction. *In* Biology of Fertilization. Vol. 3. C. B. Metz and A. Monroy, editors. Academic Press, NY. 127–165.

Kauffman, R. F., R. W. Taylor, and D. R. Pfeiffer. 1980. Cation transport and specificity of ionomycin: comparison with ionophore A23187 in rat liver mitochondria. *J. Biol. Chem.* 255:2735–2739.

Kinosita, K., Jr., H. Itoh, S. Ishiwata, K. Hirano, T. Nishizaka, and T. Hayakawa. 1991. Dual-view microscopy with a single camera: real-time imaging of molecular orientations and calcium. *J. Cell Biol.* 115:67–73.

Matsui, T., I. Nishiyama, A. Hino, and M. Hoshi. 1986a. Acrosome reaction-inducing substance purified from the egg jelly inhibits the jelly-induced acrosome reaction in starfish: An apparent contradiction. *Dev. Growth Differ.* 28:349–357.

Matsui, T., I. Nishiyama, A. Hino, and M. Hoshi. 1986b. Intracellular pH changes of starfish sperm upon the acrosome reaction. *Dev. Growth Differ.* 28:359–368.

Morris, S. J. 1990. Real-time multi-wavelength fluorescence imaging of living

cells. *Biotechniques.* 8:296–308.

Sardet, C., and L. G. Tilney. 1977. Origin of the membrane for the acrosomal process: is actin complexed with membrane precursors? *Cell. Biol. Int. Rep.* 1:193–200.

Schackmann, R. W., E. M. Eddy, and B. M. Shapiro. 1978. The acrosome reaction of *Strongylocentrotus purpuratus* sperm: ion requirements and movements. *Dev. Biol.* 65:483–495.

Schackmann, R. W., and B. M. Shapiro. 1981. A partial sequence of ionic changes associated with the acrosome reaction of *Strongylocentrotus purpuratus. Dev. Biol.* 81:145–154.

Schackmann, R. W., R. Christen, and B. M. Shapiro. 1981. Membrane potential depolarization and increased intracellular pH accompany the acrosomal reaction of sea urchin sperm. *Proc. Natl. Acad. Sci. USA.* 78:6066–6070.

Schackmann, R. W., and P. B. Chock. 1986. Alteration of intracellular [Ca^{2+}] in sea urchin sperm by the egg peptide speract: evidence that increased intracellular Ca^{2+} is coupled to Na$^+$ entry and increased intracellular pH. *J. Biol. Chem.* 261:8719–8728.

Schackmann, R. W. 1989. Ionic regulation of the sea urchin sperm acrosome reaction and stimulation by egg-derived peptides. *In* The Cell Biology of Fertilization. H. Schatten and G. Schatten, editors. Academic Press, San Diego. 3–28.

Schroeder, T. E, and R. Christen. 1982. Polymerization of actin without acrosomal exocytosis in starfish sperm: visualization with NBD-phallacidin. *Exp. Cell Res.* 140:363–371.

Suzuki, K., Y. Tanaka, Y. Nakajima, K. Hirano, H. Itoh H. Miyata, T. Hayakawa, and K. Kinosita, Jr. 1995. Spatiotemporal relationships among early events of fertilization in sea urchin eggs revealed by multiview microscopy. *Biophys. J.* 68:739–748.

Tilney, L. G., D. P. Kiehart, C. Sardet, and M. Tilney. 1978. Polymerization of Actin. IV. Role of Ca^{2+} and H$^+$ in the assembly of actin and in membrane fusion in the acrosomal reaction of echinoderm sperm. *J. Cell Biol.* 77:536–550.

Tilney, L. G., and S. Inoué. 1982. Acrosomal reaction of *Thyone* sperm. II. The kinetics and possible mechanism of acrosomal process elongation. *J. Cell Biol.* 93:820–827.

Tilney, L. G. 1985. The acrosome reaction. *In* Biology of Fertilization Vol. 2. C. B. Metz and A. Monroy, editors. Academic Press, NY. 157–213.

Trimmer J. S., R. W. Schackmann, and V. D. Vacquier. 1986. Monoclonal antibodies increase intracellular Ca^{2+} in sea urchin spermatozoa. *Proc. Natl. Acad. Sci. USA.* 83:9055–9059.

Vogel, S. S., and J. Zimmerberg. 1992. Proteins on exocytic vesicles mediate calcium-triggered fusion. *Proc. Natl. Acad. Sci. USA.* 89:4749–4753.

Watson, P. S., J. M. Plummer, and P. S. Jones. 1992. The ionophore-induced acrosome reaction differs structurally from the spontaneous acrosome reaction. *J. Exp. Zool.* 264:231–235.

Yanagimachi, R. 1988. Sperm-egg fusion. *In* Current Topics in Membranes and Transport. Vol. 32. Academic Press, NY. 3–43.